Journal of Solid Mechanics and Materials Engineering

Vol. 4, No. 4, 2010

Simultaneous Measurement of Multiple Electrical Resistance Changes with Strain of CFRP*

Kosuke TAKAHASHI**, Akira TODOROKI***
and Ryosuke MATSUZAKI***
**Tokyo Institute of Technology
Address: 2-12-1-I1-58 O-okayama, Meguro-ku, Tokyo 152-8552, Japan
E-mail: ktakahas@ginza.mes.titech.ac.jp
***Department of Mechanical Sciences and Engineering, Tokyo Institute of Technology
Address: 2-12-1-I1-58 O-okayama, Meguro-ku, Tokyo 152-8552, Japan

Abstract

Strain monitoring of CFRP structure by measuring electrical resistance change has attracted attention over the years. High electrical conductivity of carbon fibers enables to measure the strain by making electrodes on the structure's surface and using bridge circuit as conventional strain gauge. Electrical resistance change method, however, is difficult to specify the gauge length because electric current is applied directly to the structure, and the current path depends on the stacking sequences, fiber volume fraction, and electrode's location. It is also difficult to measure the electrical resistance changes at different parts simultaneously because the outputs may interfere with each other due to overlapping of current paths inside the structure. In this study, three electrodes are connected to each bridge circuit to prevent electrical interference when the electrical resistance changes are measured simultaneously, whereas electrical resistance measurements normally use two electrodes. The proposed method puts ground electrodes every other so that current path could be limited between the ground electrodes. Only the strain between ground electrodes affects the electrical resistance output, and it makes simultaneous measurements at different position possible.

Key words: Smart Materials, Stress-Strain Measurement, Monitoring, CFRP, Electrical Resistance Change Method

1. Introduction

The structural health monitoring of graphite/epoxy composites using electrical resistance change method has been an area of interest. The electrical resistance change method uses carbon fibers, the reinforcement in the composite, as sensors by utilizing their high electrical conductivity. Electrical resistance changes due to deformation or damage are detected by connecting a pair of electrodes mounted on the laminate surface to a bridge circuit, which is the same method as used by conventional strain gauges. The measurement system can be applied simply without expensive instruments and does not cause strength degradation, which might occur when embedding sensors, such as optical fiber sensors [(1)-(2)], into a material [(3)]. The electrical resistance change method has been shown to be effective in the strain monitoring of tensile loading and fiber breakage, matrix cracking, and delamination [(4)-(7)], and is expected to be applied to existing structures.

When using the electrical resistance change method, however, it is difficult to obtain

*Received 7 Jan., 2010 (No. T2-08-0504)
Japanese Original : Trans. Jpn. Soc. Mech. Eng., Vol. 74, No. 748, A (2008), pp.1573-1579 (Received 3 June, 2008)
[DOI: 10.1299/jmmp.4.557]

multipoint data simultaneously because electric current goes into the structure. If electrical currents are simultaneously applied from different points, the current paths may overlap and the resulting outputs interfere with each other. The current path depends on fiber volume fraction, stacking sequence, and electrode location because the graphite/epoxy composite has orthotropic electrical conductivity. In order to prevent electrical interference, only two adjacent electrodes are selected at any one time, with different pairs selected in series using a relay circuit. This process becomes inefficient for monitoring the whole structure as the size of the structure increases. One way to perform simultaneous monitoring is the electrical potential measurement. The electrical potential measurement forms a single electric current path between the outmost electrodes supplying the electric current and measures the potentials at every electrode within the segment. The problem is that even partial damage on the path between outmost electrodes would affect all the outputs along the path. To avoid electrical interference between simultaneously obtained outputs, each output needs to be independent from the others.

In this paper, a new electrical resistance change method is proposed. Whereas the conventional electrical resistance change method uses two electrodes for each bridge circuit, the proposed method uses three electrodes and enables multipoint measurements with independent outputs [8]. The proposed method broadens the potential application of electrical resistance measurements. For example, the multipoint measurements allow in-service structures to be diagnosed easily and reliably by the statistical method [9]. In order to demonstrate its effectiveness, the proposed multipoint measurement, the three-electrode method, is compared to the conventional two-electrode method by examining the current distribution inside a structure obtained by finite element analysis (FEA). In addition, multipoint strain monitoring is conducted on a cross-ply beam in order to confirm that the three-electrode method does not produce electrical interference.

2. Simultaneous measurements of multipoint electrical resistance changes

2.1 Inconvenience of the conventional two-electrode method

The conventional electrical resistance change method using two electrodes is illustrated in Fig. 1 and is referred to as the two-electrode method in this paper. In the figure, the electrodes to which voltage is applied are hatched and the GND electrodes are solid black. Using this method, it is difficult to specify the electric current path from the voltage applied electrode to the GND electrode owing to the orthotropic electrical properties. For example, when the electrodes are located on the surface of a cross-plied beam along the fiber direction, the main electric current paths form between the two electrodes and in a wide arc as shown in Fig. 2. Since the entire area through which electric currents flow affects the electrical resistance, deformations not only between the two electrodes but also in the arc are detected as electrical resistance changes. To perform multipoint measurements on the same surface, the amount of electric current away from the electrodes has to be small enough such that the gauge length is limited to the space between the two electrodes.

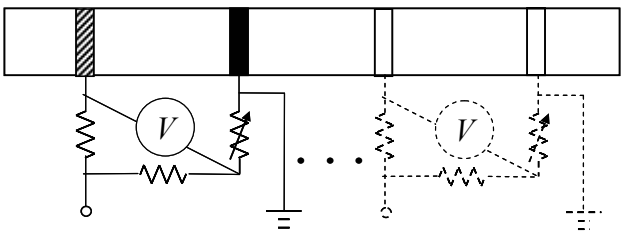

Fig. 1 Electrical resistance change method

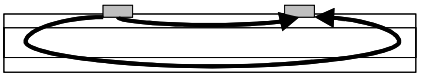

Fig. 2 Paths of electric currents

2.2 The proposed three-electrode method

The proposed three-electrode method is illustrated in Fig. 3. The electrodes are marked in the same way as for the two electrode method and are named electrode 1, electrode 2, …, and electrode 7, numbering from the left. This method differs from the two-electrode method in that three electrodes are used for each bridge circuit. Using seven electrodes, it is possible to measure three adjacent areas using bridge circuits A, B, and C as shown in Fig. 3. The electrode in the center is connected to the voltage source and the others are connected to GND.

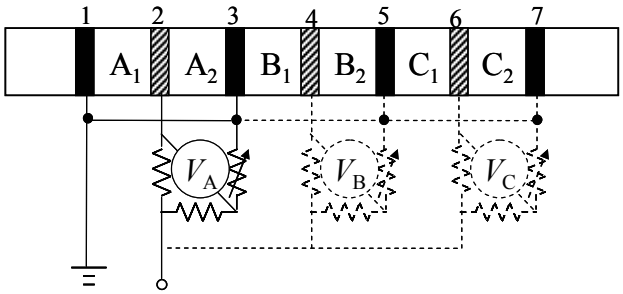

Fig. 3 Three electrode method

The electric current distribution created by bridge circuit A, which is connected to electrodes 1, 2, and 3, can be considered as the sum of distribution obtained in the two electrode method using electrodes 1 and 2 as shown in Fig. 4(a) and the distribution obtained using electrodes 2 and 3 as shown in Fig. 4(b). The arrows in Fig. 4 show the current direction and the relative amounts of electric current. The white arrows between electrodes 1 and 3 are summed, but the black arrows outside these electrodes cancel each other. As a result, the current distribution in the three-electrode method is expressed as shown in Fig. 4(c). The amount of electric current between GND electrodes is much greater than the current outside the electrodes, in comparison to the case for the two-electrode method. Since the electric current paths of each bridge circuit are divided by the GND electrodes, the electrical resistance changes are independent even if the adjacent bridge circuits share GND electrodes

By adding the third electrode, the electrical resistance between GND electrodes as part of the bridge circuit is composed of two parts connected in parallel. In bridge circuit A shown in Fig. 3, for example, the electric resistance of the part R_A is the sum of R_{A1} and R_{A2} connected in parallel if electric current outside the electrodes can be ignored.

$$\frac{1}{R_A}=\frac{1}{R_{A1}}+\frac{1}{R_{A2}} \tag{1}$$

Here, R_{A1} and R_{A2} are the electrical resistances between electrodes 1 and 2 and electrodes 2 and 3, respectively. The electrical resistances in bridge B and bridge C are expressed in the same way.

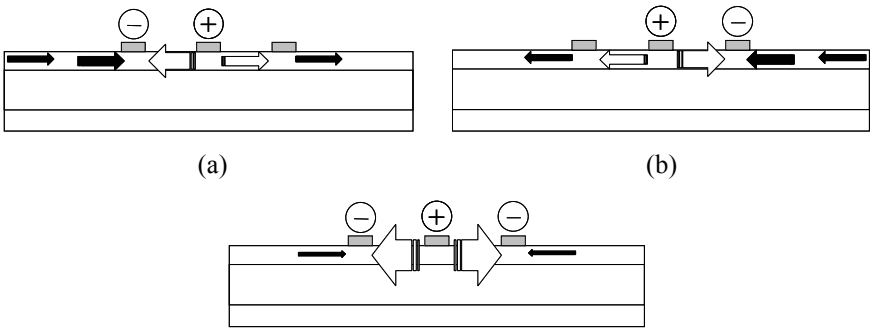

Fig. 4 Electric current density in the surface layer in the cases of (a) the two electrode method using electrodes 1 and 2, (b) the two electrode method using electrodes 2 and 3, and (c) the three electrode method using electrodes 1, 2 and 3

3. Current distribution inside the structure

3.1 Analysis

Finite element analysis is performed using the commercial software ANSYS to compare the current distribution inside a beam structure obtained by the two-electrode method with that obtained by the three-electrode method. The FEM model shown in Fig. 5 is a three dimensional beam with a length of 130 mm, width of 15 mm, and thickness of 1.6 mm. The stacking sequence is [0/90]s and the thickness of each layer is 0.4 mm. On the surface of the model, there are seven electrodes with widths of 5.0 mm each and separated from each other by 15 mm. The electrodes are numbered electrode 1, electrode 2,…, and electrode 7 counting from the left. The elements in the composite part are 0.5 mm long, 3.75 mm wide, and 0.4 mm thick. For the electric conductivity, Abry's [10] paper is referred to. The elements in the electrode part are 0.5 mm long, 3.75 mm wide and 0.2 mm thick. The electrode model aims to compensate for the difference between initial resistance of the model and experimentally measured resistances. At the interface between the electrodes and the laminate, contact resistances need to be considered. These are simply represented by the resistance of electrode model in the thickness direction. The electric conductivity of the electrode model in the direction of its thickness, σ_t, is obtained using the following equation.

$$\sigma_t = \frac{t_e}{R_C S_e} \tag{2}$$

Here, Rc is the contact resistance, S_e is the contact area of the electrode model, and t_e is the thickness of the electrode model. The contact resistance was assumed to be constant and was obtained from the resistances between two electrodes at various distances. The average of contact resistances obtained from three specimens, 106 mΩ, is used as R_C. The material properties are presented in Table 1, where 0, 90, and t represent the fiber, transverse, and through-thickness directions, respectively.

First, the current distribution inside the beam for the two-electrode method is examined. A node on the surface of electrode 3 is defined as 0 V, and electric current of 10 mA is applied to a node on the electrode 5. In addition, the distance between two electrodes is halved to confirm that the sum current distribution using the two–electrode method corresponds to that in the three-electrode method as explained in Fig. 4. Applying 10 mA to electrode 4 with electrode 3 or 5 set to 0 V, the current distributions for the two cases are summed.

Next, the current distribution for the three-electrode method is examined. Electrodes 3

and 5 are simultaneously defined as 0 V, and an electric current of 20 mA is applied to electrode 4. It should be noted the applied electric current to electrode 4 is twice of that applied in the two-electrode method since the electric current applied to electrode 4 flows to both electrodes 3 and 5.

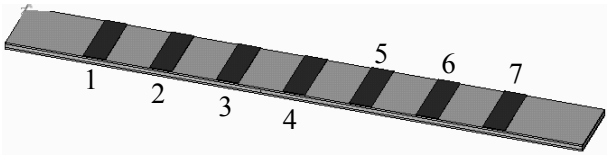

Fig. 5 FEM model

Table 1 Material properties

	Electrical conductivity [S/m]		
	0º	90º	*t*
Composite	34130	24.04	20.74
Electrode	5.959×10^{7}		25.12

3.2 Results of analysis

The current distribution for the two-electrode method using electrodes 3, 5 and using electrodes 3, 4 are shown in Fig. 6 and Fig. 7, respectively. The distribution for the three-electrode method using electrodes 3, 4 is shown in Fig. 8. The current density in the fiber direction is shown in Figs. 6(a), 7(a) and 8(a) and the current density in the thickness direction is shown in Figs. 6(b), 7(b) and 8(b). The abscissa is the longitudinal position on the surface of the beam and the ordinate is the current density. The bands in these figures represent the position of the electrodes being used.

According to the current distribution in Fig. 6, the current density outside the electrodes is rather high in both the fiber and thickness directions. This current distribution indicates an arc path of electric current. The current distribution in Fig. 7 also shows high current density outside the two electrodes even though the distance between the electrodes is reduced by half. These results show that the electric current path outside the electrodes in the two-electrode method cannot be ignored regardless of the distance between electrodes. On the other hand, the current distribution in Fig. 8 shows that the current densities outside GND electrodes is much lower compared to that for the two-electrode method shown in Figs. 6 and 7. In Fig. 8, the sum of current densities in the two-electrode method when electrodes 3 and 4 and electrodes 4 and 5 are used is also plotted, and it corresponds well to that of the three electrode method. This confirms the explanation presented in Fig. 4, that the electric density in the three-electrode method is the sum of the electric densities in the two-electrode method.

To quantitatively compare current amounts outside the electrodes in the two-electrode method, Fig. 6, with that in the three-electrode method, Fig. 8, the magnitude of current density (MCD) is calculated. In each result, the MCD outside the electrodes is obtained, and then its ratio to the total MCD is calculated. This is also calculated on the interface between the 0 degree and 90 degree layers.

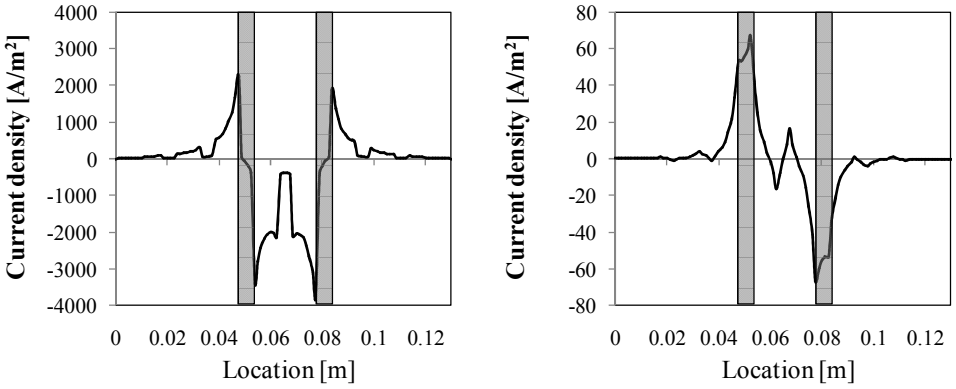

(a) (b)

Fig. 6 Current density on the CFRP surface using electrodes 3 and 5 in (a) the longitudinal direction and (b) the thickness direction

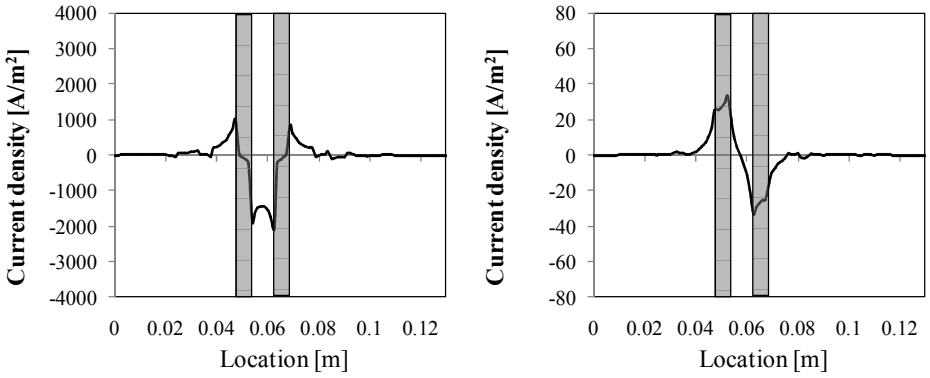

(a) (b)

Fig. 7 Current density on the CFRP surface using electrodes 3 and 4 in (a) the longitudinal direction and (b) the thickness direction

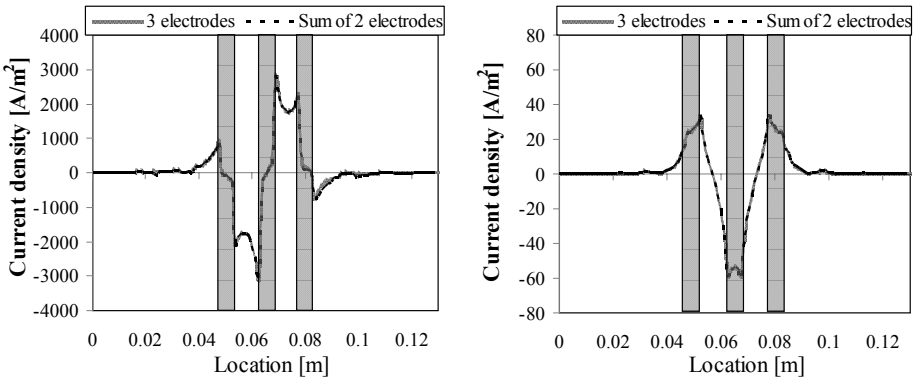

(a) (b)

Fig. 8 Current density on the CFRP surface using electrodes 3, 4 and 5 in (a) the longitudinal direction and (b) the thickness direction

The results are shown in Fig. 9. In the two-electrode method using electrodes 3 and 5, about one-third of the electric current exists outside the electrodes on the beam surface. Even on the interface between layers, the fraction of electric current outside the electrodes is about one-fourth. On the other hand, when the sum of the current densities is taken using

electrodes 3 and 4 and electrodes 4 and 5, the percentage of the electric current outside the electrodes is 23% on the surface and 20% on the interface between layers. It is shown that the summed current distribution in the two-electrode method can have less electric current outside the electrodes due to the current cancellation by different current directions. In the three-electrode method simultaneously using electrodes 3, 4, and 5, the percentage of current outside the electrodes is only 16% on the surface and 12% on the interface between layers. The amount of current outside the electrodes is even lower than that for the summed current in the two-electrode method. This means that the three-electrode method has effects other than the cancellation seen for the two-electrode method. The two-electrode method makes some electric currents divert to the bottom 0º layer in order for all the currents to reach one GND electrode. In contrast, the three-electrode method has a GND electrode on both sides of the voltage applied electrode so that electric current can go to the closer electrode without making a large arc through the bottom layer. From these results, it is shown that the proposed three-electrode method can largely decrease the electric current outside the electrodes. In other words, the area affecting the electrical resistance due to deformation can be limited to be within the GND electrodes.

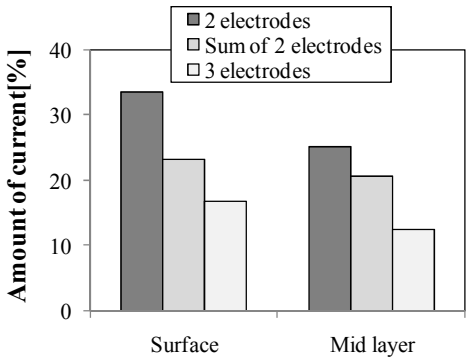

Fig. 9 Amount of electric current outside the electrodes

4. Strain monitoring with electrical resistance measurements

4.1 Specimens

In order to confirm FEA results, strain monitoring using electrical resistance change measurements is carried out with the same configuration as the analysis model. The specimen is made of unidirectional prepreg Pyrofil #380 G250 produced by Mitsubishi Rayon Co. Ltd. The stacking sequence is cross-ply of $[0_2/90_2]$s. The curing temperature is 130 °C, the curing time is 120 minutes and the pressure is 0.7 MPa under a vacuum condition. The beam is 135 mm in length, 15 mm in width, and 1.7 mm in thickness. The seven electrodes are mounted on the surface of the beam by means of the electrical copper plating method. Before the copper plating, the specimen surface is polished with sandpaper and the surface is briefly treated with concentrated sulfuric acid to remove the surface sizing of carbon fibers. This treatment improves the contact between carbon fibers and copper electrodes. After the treatment, the specimen is put into copper sulfate solution and connected to the anode of an electric power source. A copper plate is connected to the cathode and then electric current is applied. The amount of electric current is 0.7×10^{-4} A/mm^2 for 30 minutes and then 2×10^{-4} A/mm^2 for 30 minutes. The width of each electrode is 5 mm and the distance between adjacent electrodes is 15 mm. These electrodes are named electrode 1, electrode 2, …, and electrode 7, numbered from the left. The wires are soldered onto each electrode and epoxy adhesive is coated over the solder for protection.

4.2 Experiments

First, we attempt to monitor the strain change using the two-electrode method. Electrodes 3 and 5 are connected to a bridge circuit as shown in Fig. 1. The inter-laminar shear test is performed to deform the specimen. The deformation occurs only in the area between the support jigs, which are 20 mm apart. The distance between support jigs should be shorter than the distance between the electrodes connected to a bridge circuit so that only the monitored area can deform, as shown in Fig. 10. To prevent electrical contact with jigs, the jigs are covered with insulated tape. The beam specimen is compressed from the backside of the surface the electrodes are attached to, and the tensile strain at the surface is monitored. The electrical resistance between electrodes on the same surface increases in proportion to strain in the same way as conventional strain gauges do, since electric currents are mostly supplied to the surface, as shown in simulation results. The compressive speed is 0.2 mm/min and the specimen is compressed to the deflection of 0.3 mm. After the compression, the specimen is unloaded at the same speed to the initial state. The load–deflection curve obtained during the inter-laminar shear test is shown in Fig. 11. The surface strain is calculated from the deflection since there is no space for a conventional strain gauge due to the size limitation of jigs. To simply estimate the surface strain at the maximum deflection point, a linear expression is approximated from the load–deflection curve and the flexural modulus is calculated using the change ratio of the linear expression and the beam size.

$$E = \frac{1}{4}\frac{L^3}{bh^3}\frac{P}{\delta} \tag{3}$$

Here, the distance between the two support jigs is L, the specimen width is b, the specimen thickness is h, the load is P, and the deflection is δ. The stress is calculated from the following equation.

$$\sigma = \frac{3PL}{2bh^2} \tag{4}$$

Using equations (3) and (4), the strain of the specimen between the jigs is obtained.

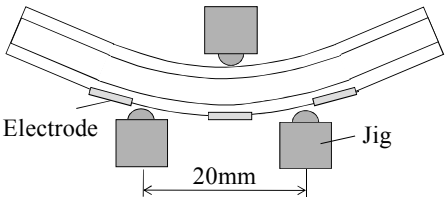

Fig. 10 Inter-laminar shear test

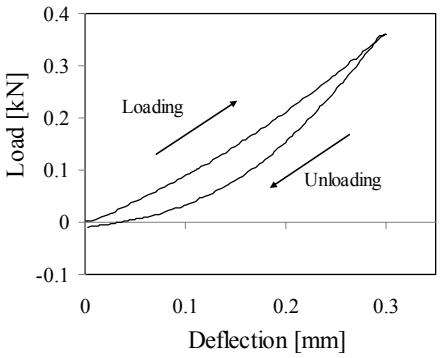

Fig. 11 Relationship between load and deflection

Second, the inter-laminar shear test is performed for the area between electrodes 1 and 3, which is outside the monitored area of the bridge circuit connected to electrodes 3 and 5. The electrical resistance change is measured to examine the influence of the current path outside the electrodes.

Next, the same experiment is performed for the three-electrode method. Electrodes 3 and 5 are connected to GND and the voltage side of a bridge circuit is connected to electrode 4. The inter-laminar shear test is performed for the area between electrodes 3 and

5, which is the monitored area of the bridge circuit, and for the area between electrodes 1 and 3, which is outside of the monitored area.

Finally, a multipoint electrical resistance measurement is performed using the three-electrode method to confirm that the method can measure the strain without any electrical interference. The seven electrodes mounted on the surface of the specimen are connected to three bridge circuits as shown in Fig. 3, and the electrical resistance changes are simultaneously measured. The inter-laminar shear test is performed on the area between electrodes 3 and 5, which is the monitored area of bridge circuit B, and the area between electrodes 1 and 3, which is the monitored area of bridge circuit A.

4.3 Results and discussion

The electrical resistance changes during the inter-laminar shear test performed on the area between electrodes 3 and 5 are shown in Fig. 12. The abscissa is the strain calculated using equations (3) and (4) and the ordinate is the electrical resistance change. The dashed line is the result for the two-electrode method and the solid line is the result for the three-electrode method. The electrical resistances for both methods increase with the tensile strain and they are very similar. Therefore, the monitoring of strain using the three-electrode method can be applied in the same way as the monitoring using the two-electrode method. The slight increase in the electrical resistance change after unloading can be considered as micro damage in the impressed part, such as matrix cracking or plastic deformation.

The electrical resistance changes when the inter-laminar test is performed outside the monitored area, between electrodes 1 and 3, are shown in Fig. 13. Compared with Fig. 12, the electrical resistance change is rather small. Still, about 2000μ is detected in the two-electrode method due to the 7000μ strain, and the electrical resistance change is unstable in both specimens. This means that deformation outside the monitored area might cause a measurement error for the monitored area. On the other hand, the electrical resistance change due to the deformation in the three-electrode method is less than half of that in the two-electrode method. Furthermore, the output is stable during the inter-laminar shear test. From these results, it is shown that the proposed three-electrode method can largely decrease the effect of deformation outside the electrodes.

The electrical resistance changes obtained by multipoint measurements using three bridge circuits are shown in Fig. 14. The solid line is the output B where the inter-laminar shear test is performed and the dashed line is the output A, which monitors un-deformed area. The output of bridge circuit B is almost the same as the results shown in Fig. 12, but the output of bridge circuit A changes little. The output neighboring the deformed area is more stable than that shown in Fig. 13. These results show that the three-electrode method can detect only the strain in the monitored area surrounded by the GND electrodes.

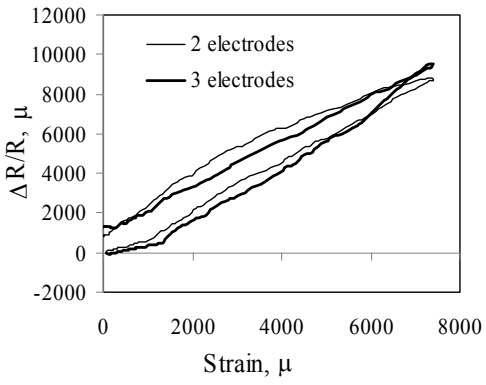

Fig. 12 ΔR/R due to deformation between electrodes 3 and 5

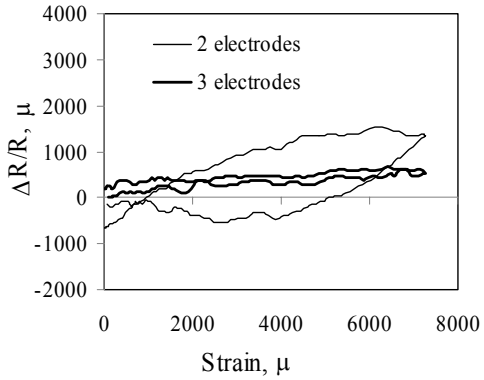

Fig. 13 ΔR/R due to deformation between electrodes 1 and 3

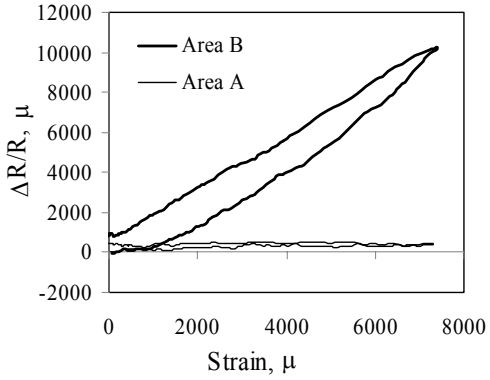

Fig. 14 ΔR/R due to deformation in the case of simultaneous measurements by the proposed method

In this paper, the target structure is a simple cross-ply CFRP beam and its study is the first step in showing the effectiveness of the proposed method. For the integration of electrodes to the existing structure, reducing the number of electrodes minimizes structural modification. This means that a setup with thin electrodes with wide spacing is desirable. The area of the electrodes may not have much influence on the measurement accuracy, but the wider spacing definitely makes the strain measurement less accurate when the strain is not uniform along the measured area. In addition, the three-electrode method requires another electrode between two electrodes to monitor the same area in the two-electrode method, and total weight of electrodes would be doubled. To minimize the amount of electrodes but retain accurate monitoring, more electrodes should be added in parts which may have complex deformation, but electrodes could be reduced in parts assumed to have uniform strain. The influence of spacing of electrodes on strain measurements needs to be investigated. Also, various stacking sequences including those with 45 degree directions and two dimensional electrode locations on panels with larger widths need to be tested. If laminates include 90 degree or 45 degree directions, electrical interference with neighboring area may occur in not only the longitudinal direction but also in the width direction. Although the effectiveness of the proposed method is shown in this paper, further consideration of the electrode location is required.

5. Conclusions

Electrical resistance measurements using three electrodes are proposed to enable the

multipoint strain monitoring on the same structure. In the proposed three-electrode method, the gauge length of each bridge circuit is limited to the space between the GND electrodes to prevent electrical interference. The current density was examined using FE analysis to compare the three-electrode method with the conventional two-electrode method, and it was shown that the amount of current outside the electrodes in the proposed method was much less than that in the conventional method. In addition, the strain monitoring of a cross-ply beam was performed during an inter-laminar shear test and the results showed that the influence of the area outside the monitored area is very little using the three-electrode method. The three-electrode method can actuate simultaneous measurements of electrical resistance change without electrical interference.

References

1. B. Lee, Review of the present status of optical fiber sensors, Optical Fiber Technology, Volume 9, Issue 2, (2003), pp. 57-79
2. Y. Fan and M. Kahrizi, Characterization of a FBG strain gage array embedded in composite structure, Sensors and Actuators A: Physical, Volume 121, Issue 2, 30 (2005), pp. 297-305
3. M. Surgeon and M. Wevers, The influence of embedded optical fibres on the fatigue damage progress in quasi-isotropic CFRP laminates, Journal of Composite Materials, 35(11), (2001), pp. 931-939
4. A. Todoroki, M. Ueda, and Y. Hirano, Strain and Damage Monitoring of CFRP Laminates by Means of Electrical Resistance Measurement, Journal of Solid Mechanics and Materials Engineering, Vol. 1 (2007) No. 8 pp. 947-974
5. A. Todoroki and M. Ueda,.Low Cost Delamination Monitoring of CFRP Beams Using Electrical Resistance Changes With Neural Networks, Smart Materials and Structures, 15 (2006) N75-N84.
6. K. Omagari, A. Todoroki, Y. Shimamura and H. Kobayashi, Detection of Matrix Cracking of CFRP Using Electrical Resistance Changes, Key Engineering Materials, Volume 297-300,(2005) pp. 2096-2101
7. A. Todoroki and J. Yoshida, Electrical resistance change of unidirectional CFRP due to applied load. JSME International J., Series A, 47,3,(2004)pp. 357-364
8. R. Matsuzaki, A. Todoroki and K. Takahashi, Time-synchronized wireless strain and damage measurements at multiple locations in CFRP laminate using oscillating frequency changes and spectral analysis, Transactions of the Japan Society of Mechanical Engineers, Series A, 72-724 (2006) pp. 1904-1911
9. K. Takahashi, A. Todoroki, Y. Shimamura, and A. Iwasaki, Statistical Damage Detection of Laminated CFRP Beam Using Electrical Resistance Change Method, Key Engineering Materials, Vols. 353-358 (2007) pp. 1330-1333
10. J. C. Abry, S. Bochard, A. Chateauminois, M. Salvia and G. Giraud,,In situ detection of damage in CFRP laminates by electrical resistance measurements, Composite Science and Technology 59 (1999) pp. 925-935